Both Ligands and Macromolecular Crowders Preferentially Bind to Closed Conformations of Maltose Binding Protein

Archishman Ghosh[†‡], Pieter E. S. Smith[†], Sanbo Qin[†‡], Myunggi Yi[§], and Huan-Xiang Zhou[†‡]*

[†] Institute of Molecular Biophysics, Florida State University, Tallahassee, Florida 30302, United States

[‡] Department of Chemistry and Department of Physics, University of Illinois at Chicago, Chicago, Illinois 60607, United States

[§] Department of Biomedical Engineering, Pukyong National University, Busan, 48513, South Korea

[*]E-mail: hzhou43@uic.edu

Supporting Information

Table S1. Parameters from fitting of titration data

Titrant	$K_{d;app}$ (μM) or K_d^C (mM)[b]	λ_f or λ_P (nm)	λ_b or λ_{CP} (nm)
Two-state model for wild-type MBP[a]			
Maltose ($[C]_T$=0)	**1.2 ± 0.1**[c]	**345.8 ± 0.1**	**350.0 ± 0.1**
Maltose ($[C]_T$=100 g/L)	1.9 ± 0.3	344.0 ± 0.1	349.8 ± 0.2
Maltose ($[C]_T$=200 g/L)	3.9 ± 0.2	343.0 ± 0.1	349.9 ± 0.1
Maltose ($[C]_T$=300 g/L)	8 ± 1	343.0 ± 0.1	350.3 ± 0.1
Ficoll ($[L]_T$=0)	**2.0 ± 0.5**	**345.6 ± 0.1**	**341.5 ± 0.4**
Three-state model for wild-type MBP[a]			
	K_d (μM) or K_d^C (mM)	λ_P (nm)	λ_b or λ_{CP} (nm)
Maltose and Ficoll	**1.3 ± 0.1**	**345.8 ± 0.1**	**350.0 ± 0.1**
	1.5 ± 0.2		**341.8 ± 0.2**
Two-state model for A96F			
Maltose ($[C]_T$=0)	**0.33 ± 0.05**	**345.9 ± 0.1**	**349.3 ± 0.1**
Maltose ($[C]_T$=50 g/L)	0.67 ± 0.05	344.0 ± 0.1	349.4 ± 0.1
Maltose ($[C]_T$=100 g/L)	0.91 ± 0.09	343.5 ± 0.1	349.2 ± 0.1
Maltose ($[C]_T$=200 g/L)	1.6 ± 0.2	342.6 ± 0.1	349.7 ± 0.2
Maltose ($[C]_T$=300 g/L)	2.2 ± 0.1	341.8 ± 0.1	349.6 ± 0.1
Ficoll ($[L]_T$=0)	**0.54 ± 0.09**	**346.1 ± 0.3**	**342.3 ± 0.2**
Three-state model for A96F			
Maltose and Ficoll	**0.42 ± 0.04**	**346.1 ± 0.1**	**349.4 ± 0.1**
	0.91 ± 0.09		**343.2 ± 0.1**
Two-state model for A96W			
Maltose ($[C]_T$=0)	**0.036 ± 0.006**	**346.5 ± 0.1**	**349.3 ± 0.1**
Maltose ($[C]_T$=100 g/L)	0.053 ± 0.003	344.0 ± 0.04	349.3 ± 0.04
Maltose ($[C]_T$=200 g/L)	0.097 ± 0.010	343.5 ± 0.1	349.1 ± 0.1
Maltose ($[C]_T$=300 g/L)	0.22 ± 0.02	343.3 ± 0.1	349.3 ± 0.1
Ficoll ($[L]_T$=0)	**0.35 ± 0.04**	**346.1 ± 0.2**	**343.6 ± 0.1**
Three-state model for A96W			
Maltose and Ficoll	**0.019 ± 0.002**	**346.4 ± 0.1**	**349.3 ± 0.1**
	0.47 ± 0.05		**343.2 ± 0.1**
Two-state model for I329W			
Maltose ($[C]_T$=0)	**0.014 ± 0.009**	**346.4 ± 0.04**	**349.7 ± 0.03**
Maltose ($[C]_T$=100 g/L)	0.030 ± 0.006	344.4 ± 0.1	350.1 ± 0.1
Maltose ($[C]_T$=200 g/L)	0.056 ± 0.011	344.4 ± 0.1	350.6 ± 0.1
Maltose ($[C]_T$=300 g/L)	0.12 ± 0.01	343.6 ± 0.1	350.8 ± 0.1
Ficoll ($[L]_T$=0)	**0.65 ± 0.11**	**346.4 ± 0.2**	**343.1 ± 0.2**

Three-state model for I329W			
Maltose and Ficoll	**0.012 ± 0.002**	**346.4 ± 0.1**	**349.7 ± 0.1**
	0.70 ± 0.11		**343.2 ± 0.1**
Two-state model for A96W/I329W			
Ficoll ($[L]_T$=0)	0.45 ± 0.11	348.9 ± 0.3	345.9 ± 0.3
Two-state model for MBP-NBD in Ficoll70			
	$K_{d;app}$ (μM)		
	Peak wavelength with 280 nm excitation	Fluo. intensity at 550 nm with 500 nm excitation	
Maltose ($[C]_T$=0)	5.8 ± 0.4	29 ± 1	
Maltose ($[C]_T$=50 g/L)	14 ± 1	30 ± 1	
Maltose ($[C]_T$=100 g/L)	30 ± 2	61 ± 1	
Maltose ($[C]_T$=200 g/L)	61 ± 3	145 ± 3	
Two-state model for MBP-NBD in BSA			
Maltose ($[C]_T$=0)		26 ± 0.7	
Maltose ($[C]_T$=50 g/L)		219 ± 14	
Maltose ($[C]_T$=100 g/L)		469 ± 22	

[a]Taken from Miklos et al. (2013).

[b]$K_{d;app}$ (μM) applies to rows where maltose is the titrant; K_d^C (mM) applies to rows where Ficol70 is the titrant.

[c]Bold entries are obtained in both two-state and three-state fits. Whereas the two-state model was used to independently fit five or six titration curves, the three-model in essence provides a constrained, simultaneous fit of all these titration curves. The degree of agreement between the corresponding parameters in the two- and three-state fits is thus a measure of the soundness of the three-state competitive model.

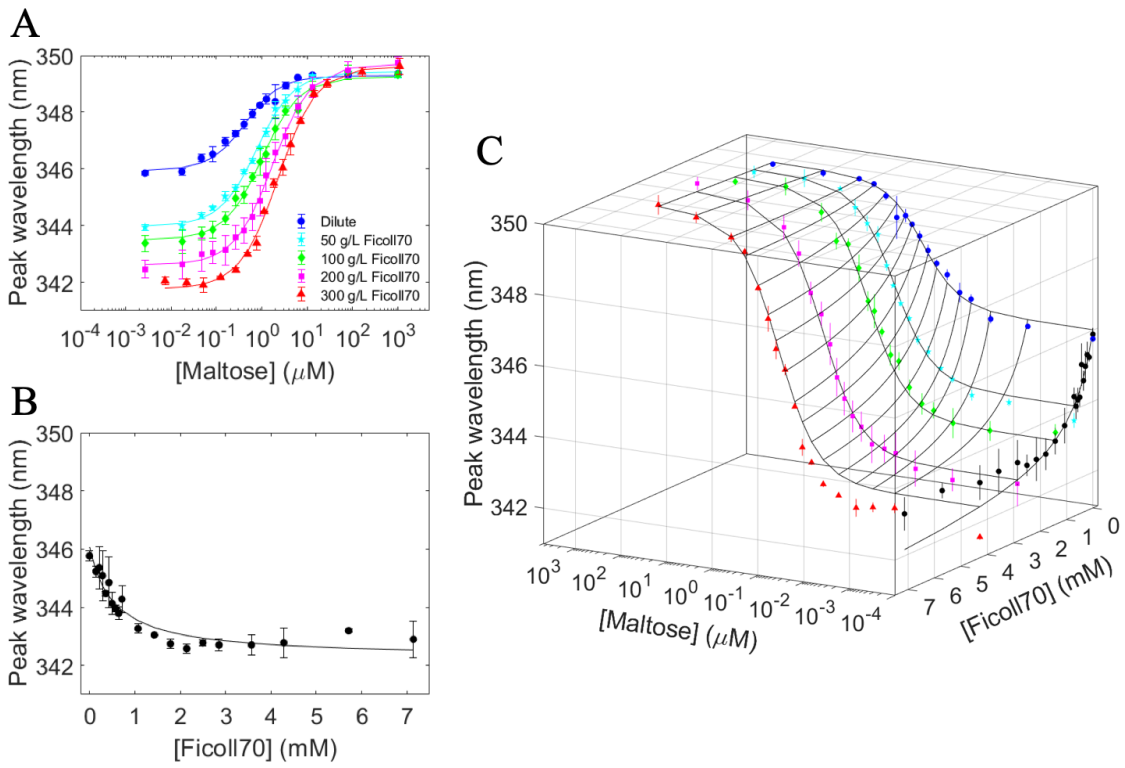

Figure S1. (A) Two-state fit of binding isotherms from titrating maltose into the A96F mutant in the absence or presence of fixed concentrations of Ficoll70. (B) Two-state fit of the binding isotherm from titrating Ficoll70. (C) Three-state fit of all the binding isotherms.

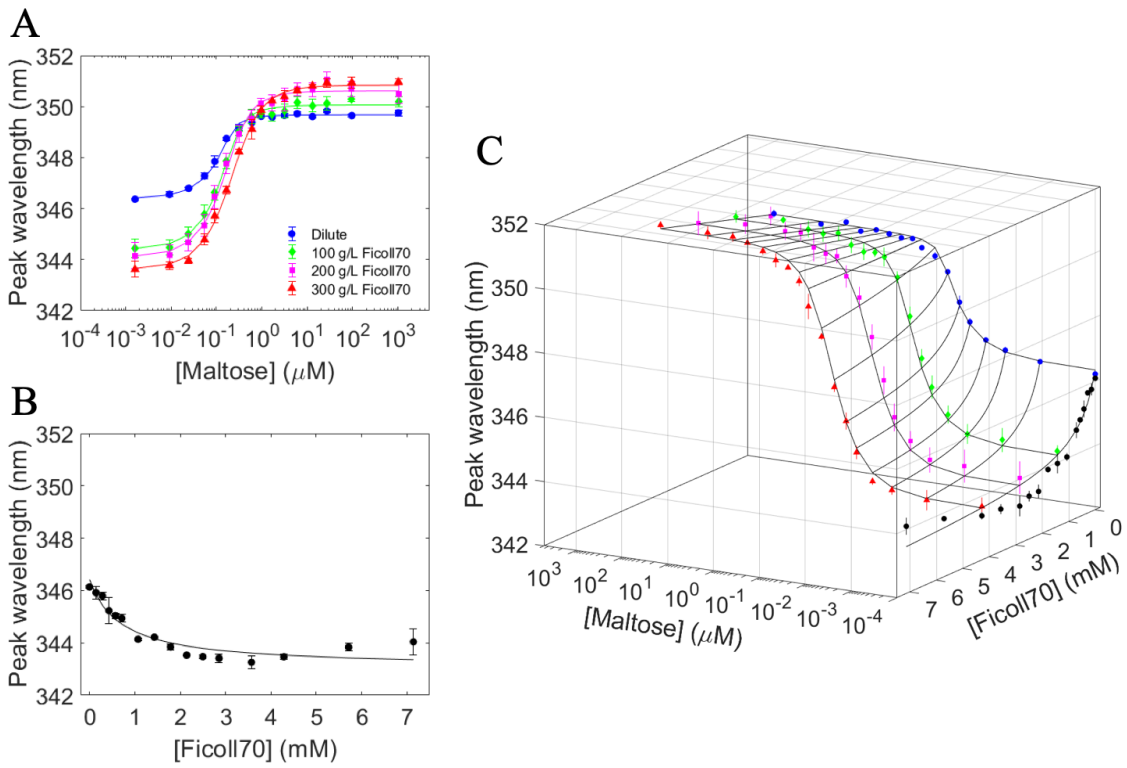

Figure S2. (A) Two-state fit of binding isotherms from titrating maltose into the I329W mutant in the absence or presence of fixed concentrations of Ficoll70. (B) Two-state fit of the binding isotherm from titrating Ficoll70. (C) Three-state fit of all the binding isotherms.

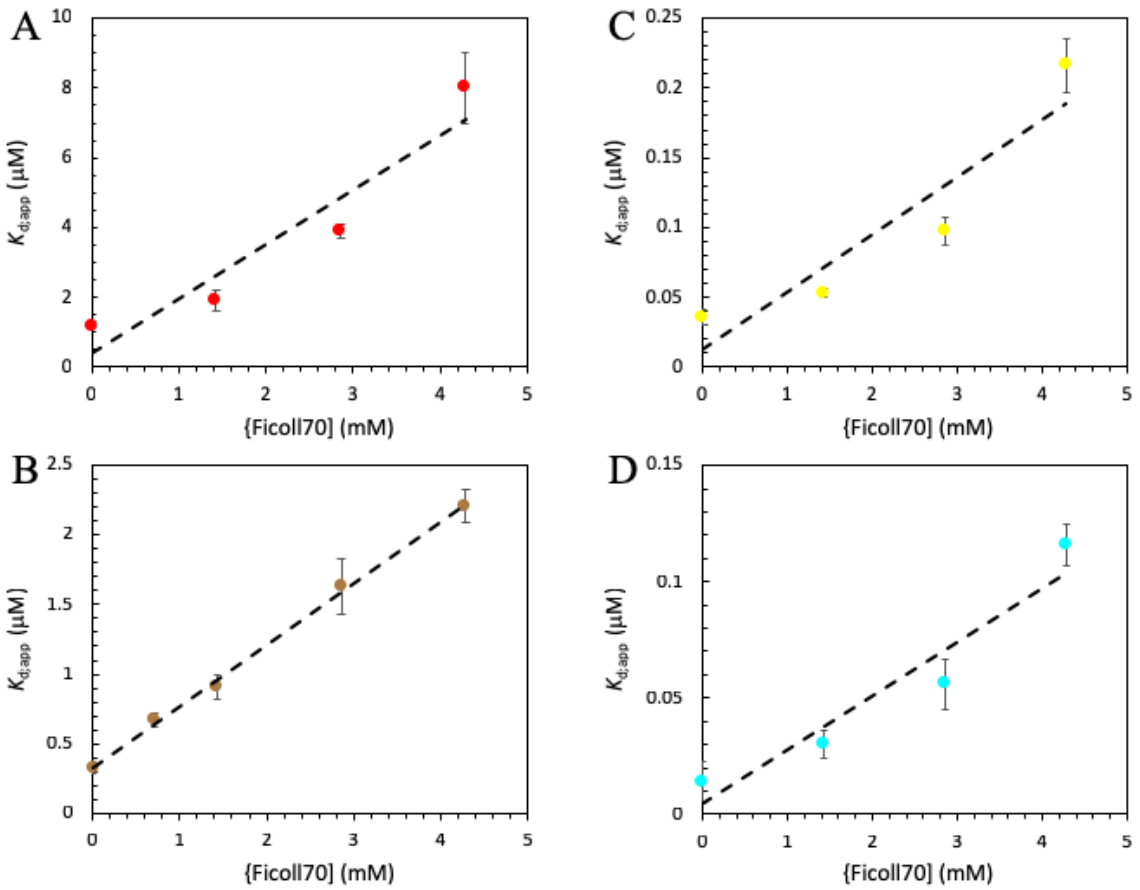

Figure S3. Linear dependence of the apparent maltose dissociation constants on Ficoll70 concentration, expected for a three-state competitive model. (A) Wild-type MBP. (B) A96F mutant. (C) A96W mutant. (D) I329W mutant.

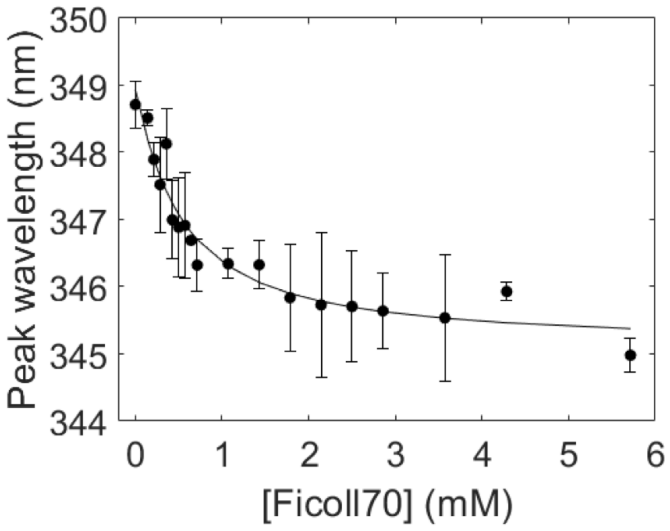

Figure S4. Two-state fit of the binding isotherm from titrating Ficoll70 into the A96W/I329W mutant.

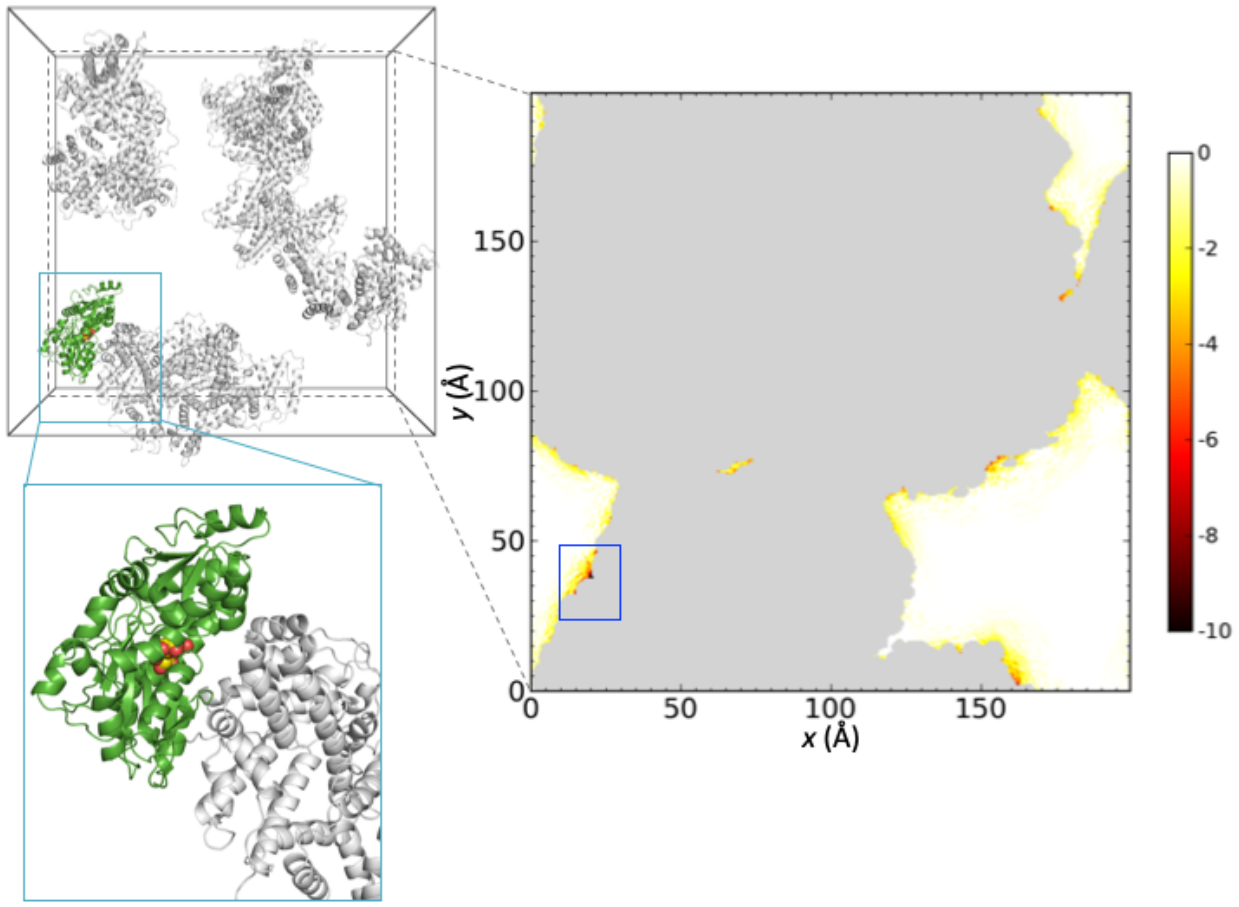

Figure S5. FMAP calculation of the protein-crowder interaction energies. An MBP molecule (green) is fictitiously placed into many locations inside a cubic box with side length of 200 Å containing eight BSA molecules (gray), representing a concentration of 110 g/L. The interaction energies within a slice of the crowder solution are displayed as colors according to a scale (in kcal/mol) shown on the right. The particular MBP molecule displayed is within a "hot" region (center of blue rectangle). An enlarged view of the pose with this MBP molecule docked to a neighboring BSA molecule is shown at lower bottom.

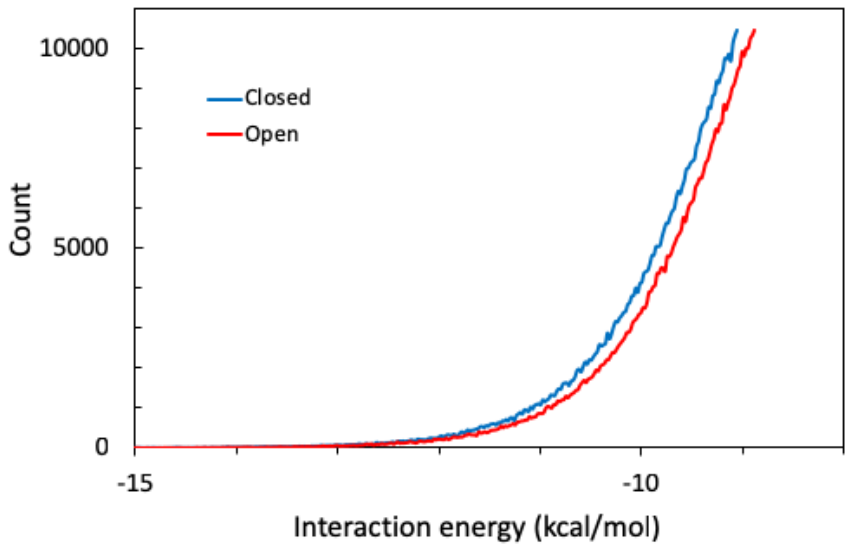

Figure S6. Histograms of MBP-BSA pairwise interaction energies. MBP is either in the closed form (blue curve) or open form (red curve). By the FMAP method, 2×10^6 MBP placements in a box of BSA molecules with the lowest interaction energies were obtained. Out of these, the interaction energies were further calculated by an atom-based method and the results were collected for 1.52×10^5 MBP placements (the remaining placements were newly found to have clashes with the crowders). The latter results were grouped into bins with 0.02 kcal/mol width, and the count in each bin is displayed.